J Wood Sci (2011) 57:119–125
DOI 10.1007/s10086-010-1151-0

ORIGINAL ARTICLE

Jung-Pyo Hong · J. David Barrett · Frank Lam

Three-dimensional finite element analysis of the Japanese traditional post-and-beam connection

Received: May 12, 2010 / Accepted: August 11, 2010 / Published online: January 4, 2011

Abstract A three-dimensional finite solid element model for Japanese traditional post-and-beam connections was developed using the wood foundation method, which employed the concept of a beam on a nonlinear foundation. The wood foundation in the model was a three-dimensionally prescribed zone surrounding a nail shank in order to address the intricate wood crushing behavior induced by nail slip. Material models for the wood members and the foundation were developed based on the transversely isotropic plasticity from the software package ANSYS. The Japanese post-and-beam connection modeled was a ten-nail multiple connection with a mortise and tenon joint and is called the CPT (Corner Plate, T-shaped) connection. Details of the model development are presented. As a feasibility study, blind predictions of the model were compared with available connection test data and showed good results for predicting the progress of the load–deformation relations in three dimensions. However, the limitation of the model was found in simulating fracture failures such as wood splitting or nail tear-out from the wood. Model applications and the need for model improvement are discussed.

Key words Three-dimensional finite element model · Nailed connection · Wood mechanical properties

Introduction

Utilization of Canadian wood species for Japanese traditional post-and-beam construction has been comprehensively studied over past 10 years at the University of British Columbia (UBC), Canada.[1,2] As a part of the studies, the development of three-dimensional finite element (FE) models for the Japanese traditional post-and-beam connections was initiated. The objective of the modeling work was to develop deeper understanding on three-dimensional (3D) stress states in a complicated connection system in an effort to develop innovative solutions for improving the Japanese traditional connection method with Canadian wood products. Since the traditional post-and-beam connection includes the interaction of the mortise and tenon joint and the nailed connections, FE analysis with solid elements was considered the best approach to investigate the behavior of the connection under loads.

However, the lack of current techniques in finite solid element modeling for wood materials in connections necessitated an original study to develop a 3D FE model for nailed connections because the Japanese post-and-beam connection includes multiple-nail connections with a T-shaped side metal plate.

To date, 3D FE models of wood connections have focused mainly on bolted connections because the crushing (or compression) behavior of wood under a bolt with a relatively large diameter was assumed to follow the conventional mechanical properties of wood that were determined through uniaxial compression tests.[3–7] However, this assumption is not applicable for nailed connections because the interaction between the nail and the wood is governed primarily by the crushing behavior of the local wood contacting the nail rather than by the gross compression behavior of the wood.[8]

Recently, a 3D FE modeling method that is capable of accounting for wood crushing behavior, called the 3D wood foundation model, was introduced by Hong et al.[9,10] A model using a 3D wood foundation for single-nailed connections showed good agreement in the ramp load–deformation curves and the deformed shapes. In this study, therefore, a feasibility study of the finite solid element model for multiple-nailed connections was conducted with the Japanese traditional post-and-beam connection, called the CPT (Corner Plate, T-shaped) connection. Blind predic-

J.-P. Hong[1] (✉) · J.D. Barrett · F. Lam
Department of Wood Science, University of British Columbia, Vancouver, BC V6T IZ4, Canada

Present address:
[1]Building Systems, FPInnovations, 2665 East Mall, Vancouver, BC V6T IW5, Canada
Tel. +1-604-222-5624; Fax +1-604-222-5690
e-mail: jungpyo_hong@hotmail.com

Part of this article was presented at the 10th World Conference on Timber Engineering

tions of the model were compared with the test data of the CPT connection that were available from a previous test program at the University of British Columbia.[1,11] All relevant FE analyses in this study were performed using the commercial software package, ANSYS

Theory

Three-dimensional wood foundation model in dowel-type wood connections

Foschi and Bonac[8] developed the wood foundation method for modeling a dowel-type wood connection that treats the wood under the connector as a nonlinear foundation. In this study, the three-dimensional wood foundation method introduced by Hong et al.[9,10] was used for modeling the nailed connections of the CPT connection. The three-dimensional wood foundation is a prescribed zone surrounding a nail shank. Figure 1 shows a half-size analog of the wood foundation used for a nail-embedment solid element model. The foundation material parameters were determined through nail-embedment tests, and then the parameters were assigned to the prescribed foundation zone in order to account for the load–wood crushing (embedment) behavior.

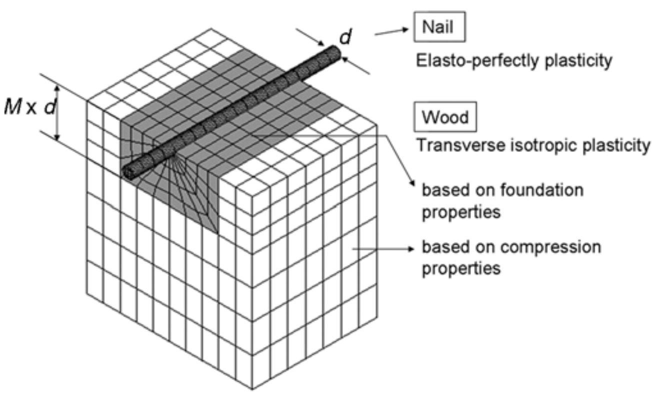

Fig. 1. Conceptual illustration for the wood foundation model in the three-dimensional finite element nail-embedment model. d is the diameter of the nail, M is the multiplier for determining the depth ($M \times d$) of the wood foundation

Material parameters for the 3D FE models for the wood and wood foundation

The procedures for determining the material parameters used for the 3D wood foundation method are introduced in Table 1. The transversely isotropic plasticity model with bilinear stress–strain relations, as used by Moses,[4,5] was adopted for 3D FE material modeling of the wood and wood foundation. This model was implemented through the TB,ANISO option in ANSYS, which is based on Hill's potential theory and an associative flow rule.[4,5,12] Based on compressive strength properties, equality of bilinear stress–strain relationships in tension and compression was assumed.[4–7] Transversely averaged Poisson's ratios taken from the literature were used.[13] Yield points in the bilinear stress–strain relationships were determined by bilinear curve fitting to the load–deformation curves from wood compression tests.

For the wood foundation, the bilinear stress–strain relationships were derived from the nail-embedment curves parallel and perpendicular to the grain direction as illustrated in Fig. 2. The nominal bilinear stress–strain relations for the foundation were calculated by:[9,10]

$$\sigma_{\text{nom.}} = \frac{P_y}{d} \tag{1}$$

$$\varepsilon_{\text{nom.}} = \frac{W_y}{d} \tag{2}$$

$$K = \frac{\sigma_{\text{nom.}}}{\varepsilon_{\text{nom.}}} = \frac{P_y}{W_y} \tag{3}$$

where σ_{nom} is the nominal yield stress of the wood foundation (MPa); ε_{nom} is the nominal yield strain of wood foundation (mm/mm); K is the nominal foundation modulus (MPa); d is the diameter of the dowel (nail) shank (mm); P_y is the yield load in the bilinear load/unit length–embedment curve (N/mm); and W_y is the yield deformation in the load/unit

Table 1. Procedures for determining the material parameters of the three-dimensional (3D) finite element (FE) models for the wood and wood foundation

Requisite constant	Symbol	Direction	Method of determination
Initial modulus	E	L, R, T	Compression test, or dowel embedment test
Initial shear modulus	G	RL, LT, RT	Coupled bilinear constitutive model[a]
Poisson's ratio	ν	RL, LT, RT	Average values from the literature[b]
Tensile yield strain	ε_y	L, R, T	Equal to compressive properties
Tensile tangent modulus	E^t	L, R, T	Equal to compressive properties
Compressive yield strain	ε_y	L, R, T	Compression test, or dowel embedment test
Compressive tangent modulus	E^t	L, R, T	0.01 × initial modulus (E)
Shear yield strain	γ_y	RL, LT, RT	Coupled bilinear constitutive model[a]
Shear tangent modulus	G^t	RL, LT, RT	0.01 × initial shear modulus (G)

The parameters in R and T directions are equal according to the transversely isotropic plasticity
L, longitudinal; R, radial; T, tangential
[a]The theoretical models developed by Saliklis et al.[15]
[b]In this study, the values from the Wood Handbook[13] were cited, except for the computed Poisson's ratio as $\nu_{TL} = \nu_{LT} \cdot (E_T/E_L)$

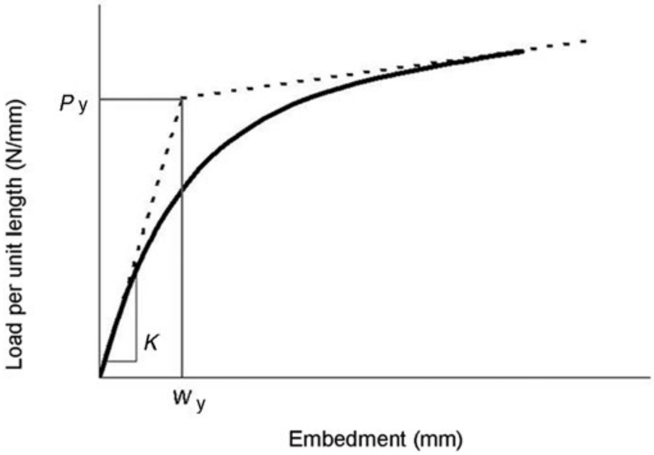

Fig. 2. Example of a load per unit length–embedment curve

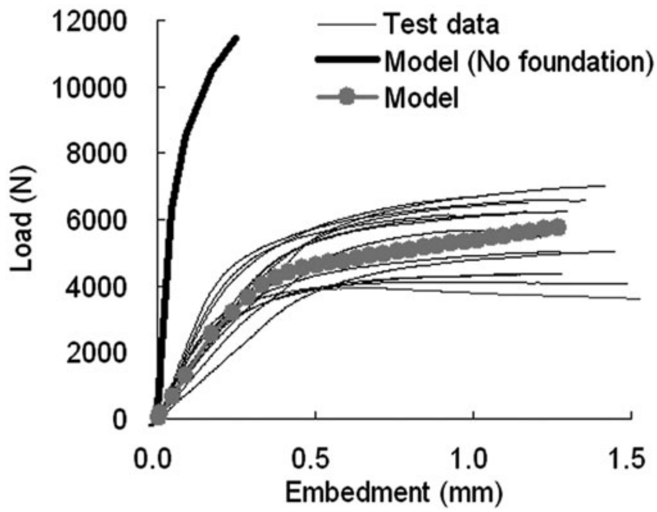

Fig. 3. Simulated and tested load–nail embedment curves in parallel-to-grain direction for a nail diameter of 3.3 mm and a wood specimen 38 mm thick. The no-foundation model used only conventional wood material parameters derived from uniaxial compression tests. This resulted in an unacceptably stiff curve

length–embedment curve (mm). For the nominal yield stress and strain, the diameter of the nail shank (d) was chosen to normalize the dimensions of variables involved since the diameter of the nail shank was presumed to be the most important nonmaterial factor governing the localized wood crushing behavior. Note that Eq. 1 for the nominal yield stress is the same form as given for calculation of dowel-embedment strength in ASTM D 5764.[14] Once the nominal foundation properties are determined, these should be calibrated to become the effective properties depending on the geometry of the foundation. For shear strength properties of the wood and wood foundation, shear moduli and shear yield points were estimated using the theoretical relationship given by Saliklis et al.:[15]

$$\text{Initial shear modulus: } G_{ij} = G_{ji} = \frac{\sqrt{E_i \cdot E_j}}{2 \cdot \left(1 + \sqrt{\nu_{ij} \cdot \nu_{ji}}\right)} \tag{4}$$

$$\text{Shear yield strain: } \left(\gamma_{\mathrm{y}}\right)_{ij} = \left(\gamma_{\mathrm{y}}\right)_{ji} = \frac{(\sigma_{\mathrm{int.}})_i}{1.98 \cdot E_i} \cdot \sqrt{\frac{E_i}{G_{ij}}} \tag{5}$$

where i, j are the parallel-to-grain (L) or perpendicular-to-grain (T) direction; E is the initial modulus (compressive modulus of elasticity, or effective foundation modulus (MPa); G is the initial shear modulus) (MPa); ν is Poisson's ratio; γ_y is the shear yield strain in the bilinear shear stress–strain curve (mm/mm); and $\sigma_{\mathrm{int.}}$ is the stress intercept in the bilinear normal stress–strain curve (MPa). The tangent moduli in compression and shear were taken empirically as a value of 0.01 × initial modulus. Depending on the dimension of the prescribed foundation, the nominal foundation modulus (K) and yield strain ($\varepsilon_{\mathrm{nom.}}$) should be calibrated to the effective foundation properties in initial modulus (E) and yield strain (ε_y), as shown in Table 1. The effective foundation properties were determined according the calibration procedures given by Hong et al.[9,10] These effective foundation properties should enable the 3D FE nail-embedment model to simulate the load–embedment curves in parallel- and perpendicular-to-grain directions simultaneously (e.g., see Fig. 3).

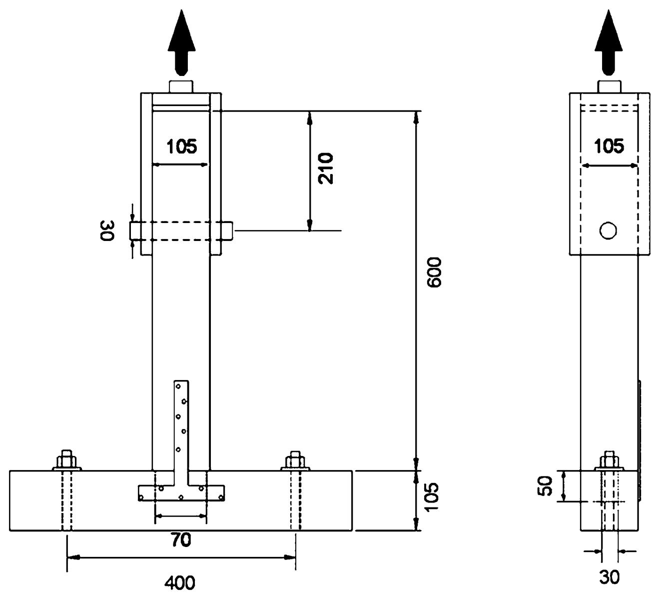

Fig. 4. An example of the Japanese post-and-beam connection test carried out in a University of British Columbia research program (units: mm)

Materials and methods

The Japanese CPT connection is a standard connection for attaching a post to a beam in Japanese traditional post-and-beam construction. This connection consists of a T-shaped steel plate connector, called a CPT metal plate, with ten Japanese standard nails. Often, a mortise and tenon joint is combined to strengthen the connection. Figure 4 shows the CPT connection and the test setup used for the tension test in the UBC research program.[1,11] The test configuration and

Table 2. Material parameters of 3D FE model using Douglas fir

	Initial modulus, E_L (MPa)	Initial modulus, $E_R = E_T$ (MPa)	Yield stress σ_L (MPa)	Yield stress $\sigma_R = \sigma_T$ (MPa)	Poisson's ratio ν_{LT} ( )	Poisson's ratio ν_{RT} ( )
Wood	16900	832	43.9	5.03	0.37	0.38
Wood foundation	736	142	16.0	6.53	0.37	0.38

L, R, and T represent longitudinal, radial and tangential directions, respectively

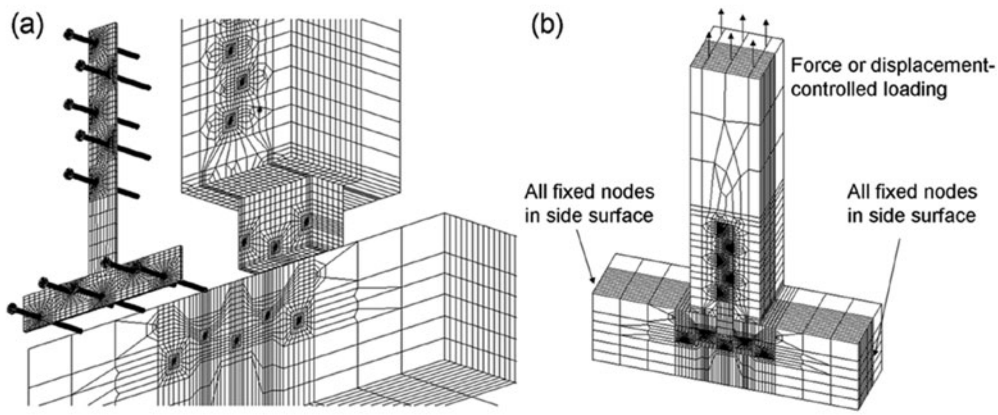

Fig. 5. Three-dimensional finite element CPT (Corner Plate, T-shaped) connection model (**a**) and the boundary conditions (**b**)

the results were used for the blind prediction of the 3D FE model. A CPT metal plate was installed with ten Japanese standard ZN65 nails (hand driven) on one side of a post-and-beam member with a 105 mm × 105 mm cross section. The wood members of the UBC connection specimens were Canadian coastal Western Hemlock (*Tsuga heterophylla*), which had a range of specific gravities (SG) from 0.39 to 0.47. In this feasibility study, however, the CPT connection model was developed with Douglas fir (*Pseudotsuga menziesii*, average SG = 0.54), on which the development of the original wood foundation model had been based.[9,10] Further studies should be considered for the generalized use of the model with other wood species. Douglas fir wood, conditioned to a moisture content of 15%, was used for the material property tests. According to ASTM D 143, the compression tests were conducted using a 25-mm wide × 25-mm thick × 100-mm high wood specimen in the longitudinal, radial, and tangential direction, respectively, with 45 repetitions. Also, for the material properties of the wood foundation, nail-embedment tests were conducted using Japanese standard nail ZN65, which has a shank diameter of 3.3-mm and a length of 65-mm. The tests were done in longitudinal, radial, and tangential directions with 15 repetitions, respectively, according to the ASTM D 5764 half-hole embedment test. The final material parameters for the model input of the wood and wood foundation are summarized in Table 2. For the material model of nails, an elasto–perfectly plastic model was assumed with a yield stress of 360 MPa, a modulus of 200 GPa, and a Poisson's ratio of 0.3.[9] For the CPT plate connector, a yield stress of 250 MPa, a Young's modulus of 200 GPa, and a Poisson's ratio of 0.3 were used.[1,11]

Finite solid element modeling

The dimensions and boundary conditions of the CPT connection model followed the UBC test configuration as shown in Fig. 4. No influence from loose or tight wood-to-wood contact in the mortise and tenon joint was considered.

To embody the connection, eight-noded, quadrilateral isoparametric brick elements (SOLID45 from ANSYS) were used. The surface-to-surface contact elements were defined on every contact interface with a frictional coefficient of 0.7 for wood-to-wood and wood-to-steel contacts, and 0.3 for steel-to-steel contact (CONTA174 and TARGE170 from ANSYS).[4,16] Figure 5 shows the solid element model with the post-and-beam member, the nails, and the plate connector separated, and a description of boundary conditions.

The size of the wood foundation was chosen to have a square cross section with a depth of 4.5 × 3.3-mm nail diameter ($M \times d$ as shown in Fig. 1). The selection of the multiplier as 4.5 was based on the efficiency of solution convergence for the simulation of nail-embedment behavior studied by Hong et al.[9,10] Since the nail spacing of the connection was narrow, two adjacent foundations overlapped partly. A wood foundation with a square cross section facilitated the meshing on the overlapping regions.

Results and discussion

Deformation and failures of the CPT connection

Figure 6 shows the progress of the simulated deformation when displacement-controlled, and force (pressure)-con-

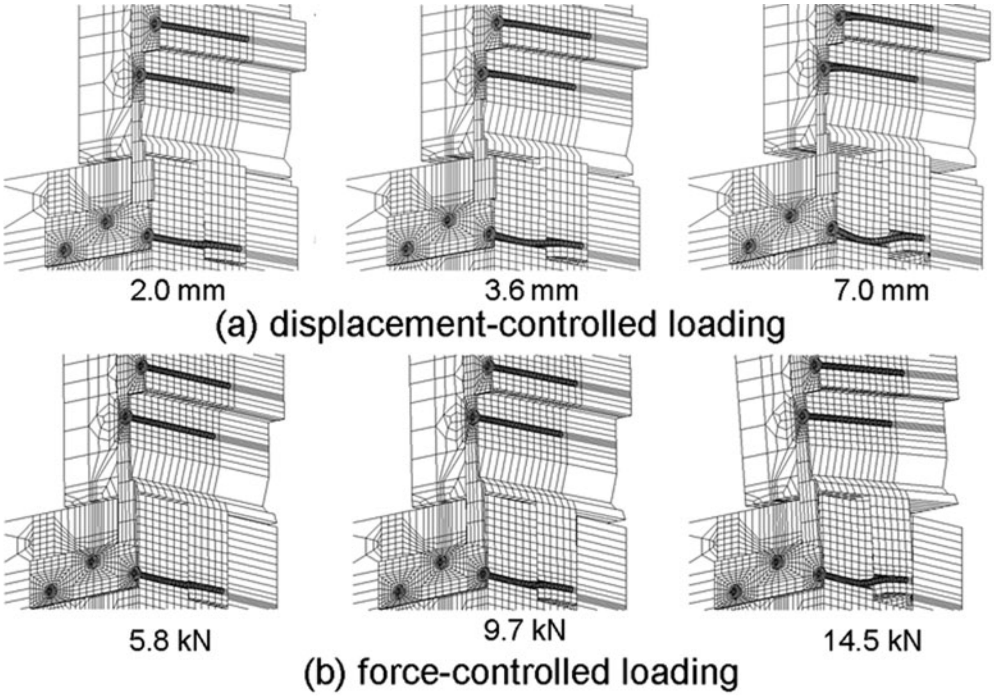

Fig. 6. Simulated displacement (sectioned views) of the CPT connection on **a** displacement-controlled loading and **b** force-controlled loading

Fig. 7. Actual failure modes of the CPT connection under tension: **a** splitting on tension perpendicular to the grain, **b** nail pull-out and CPT plate in shear on a specimen with a short tenon[1,2]

trolled loading were applied. The displacement-controlled loading has all nodes on the top surface of the post uniformly displaced in the direction parallel to the post, while in the force-controlled loading, the applied forces always acts in a direction normal to the top surface of the post, wherever the post moves.

The simulated deformation using displacement-controlled loading showed better agreement with the actual deformation shown in Fig. 7. The difference resulting from the different loading methods in the simulated deformation was the tilting behavior of the post member. The model using incremental displacement-controlled loading showed a uniformly vertical translation of the post member while the force (pressure)-controlled loading represented the tilting behavior (see Fig. 6b). This tilting behavior did not agree with the actual deformation. The simulated results using the force-controlled loading were, therefore, abandoned for analysis purposes.

Figure 8 shows the simulated deformation of nails and CPT plate under displacement-controlled loading. The simulated flexural deformation of the three nails penetrating the tenon agreed well with the observed nail pull-out from the bottom sill and intensively plastic bending shown in Fig. 7b. Also, the simulated plastic strain contours in Fig. 8b show a good indication of the progress of the plate shear failure.

Modified model

The major failure modes of the CPT connection were perpendicular-to-grain tension splitting of the beam member, the nail pull-out, and the plate shear. However, during the process of model development, it was discovered that the most influential failure on model prediction was the nail tear-out from the tenon as, shown in Fig. 9.

In the CPT connection, the three middle nails of the five nails in the beam member penetrated the tenon. In this

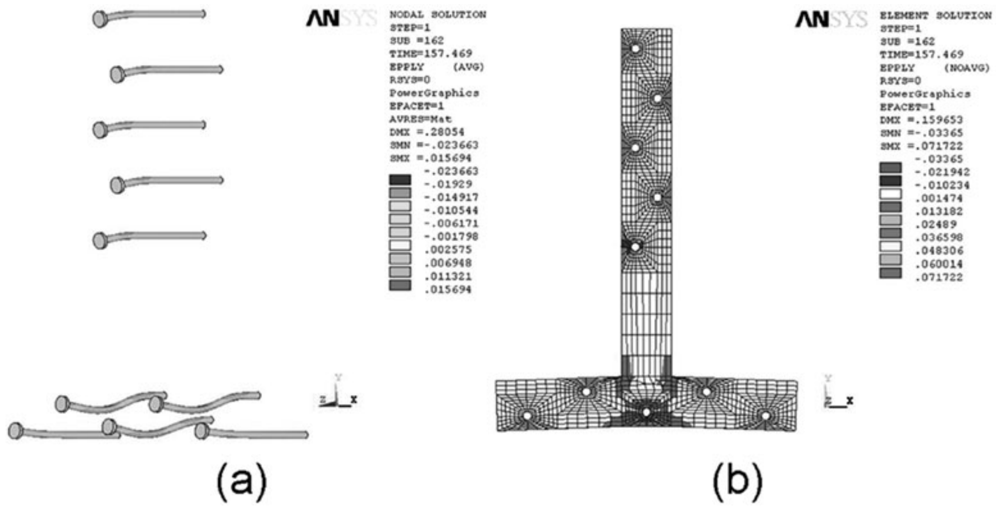

Fig. 8. The Y-directional plastic strain contours in the nails (**a**), and the CPT plate (**b**)

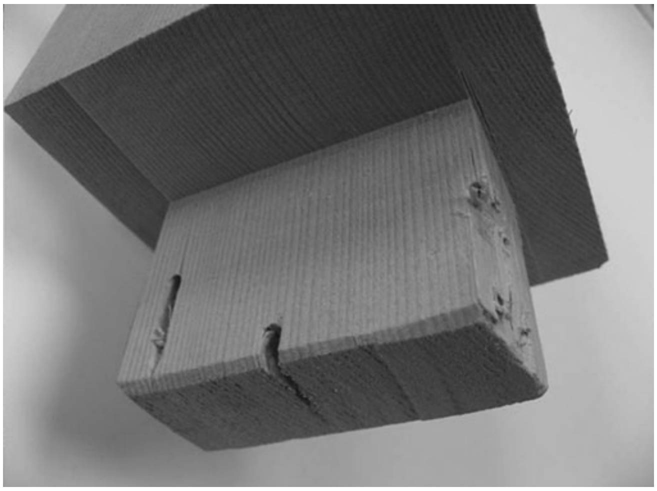

Fig. 9. Typical failure modes of the three nails penetrating the tenon: nail tear-out from tenon

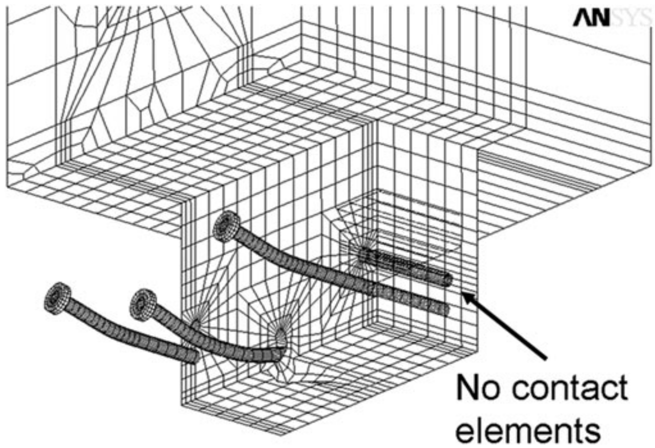

Fig. 10. Simulated deformed shape of the modified CPT connection model

configuration, the three nails had a narrow end or edge distance in the tenon. Therefore, it is most likely that the failures of the nail connections within the tenon occurred in a brittle manner, including the edge splitting of the side nails and the tear-out of the centre nail. These kinds of failures may occur at the initial deformation level, or even when a nail is driven improperly. Once a nail is pulled out of the tenon, the load-carrying ability of the nail connection within the tenon vanished. The model, however, could not simulate this kind of fracture process. This is a limitation of the model in this study. As shown in Fig. 10, the wood elements surrounding the centre nail could not split off unless a fracture algorithm or an intentional cleavage for allowing the tear-out was introduced into the model. As long as the nail was surrounded by wood elements, the load-carrying ability of the connection was retained in the model. In order to investigate the influence of these initial fractures on the simulation, the original CPT connection model was modified to remove the load-carrying ability of the side nail connections in the tenon, by eliminating the contact elements between the side nails and the tenon. The nails could then move independently, regardless of the surrounding wood elements in the tenon. The centre nail connection model remained without any modifications.

Simulated load–deformation curves

The load–deformation curves simulated using the original and modified connection models are superimposed on the test data in Fig. 11. Note that the two black bold curves in Fig. 11 are the test data of the CPT connection with a short tenon that the three middle nails did not penetrate (see the tenon in Fig. 7b). In the tests and the simulation, the three middle nail penetrations seem to significantly influence the initial stiffness or the load-carrying capacity of the connection, although the existence of the initial fracture in the real tenon was unknown. This implies that if 3D FE parametric and stress-quantitative studies are conducted for optimizing the configuration of the CPT connection, some improvement for the connection performance should be explored.

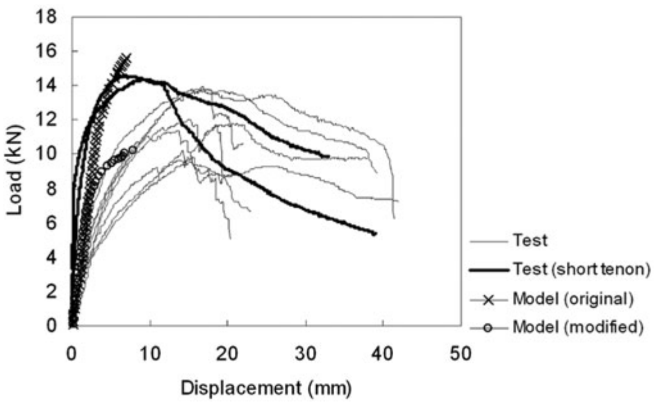

Fig. 11. Simulated load–deformation curves of the initial and the modified CPT connection model

Conclusions

A three-dimensional finite element model of a Japanese traditional post-and-beam connection with multiple-nail connections and a wood-to-wood joint was developed using the three-dimensional wood foundation approach. This three-dimensional model showed a good ability to reveal the internal behavior of the connection. Simulated results that can be quantified three-dimensionally in terms of stress and strain would lend themselves to the improvement of dowel-type wood connections.

References

1. Stefanescu M (2000) Lateral resistance of traditional Japanese post-and-beam frames under monotonic and cyclic loading conditions. Master's thesis, Department of Wood Science, The University of British Columbia, Vancouver
2. Li M (2009) Seismic performance of post-and-beam wood buildings. Ph.D. dissertation, Department of Wood Science, The University of British Columbia, Vancouver
3. Patton-Mallory M (1996) The three-dimensional mechanics and failure of single-bolt wood connections. Ph.D. dissertation, Colorado State University, Fort Collins
4. Moses DM (2000) Constitutive and analytical models for structural composite lumber with applications to bolted connections. Ph.D. dissertation, Department of Civil Engineering, University of British Columbia, Vancouver
5. Moses DM, Prion HGL (2004) Stress and failure analysis of wood composites: a new model. Composites Part B 35:251–261
6. Kharouf N (2001) Post-elastic behaviour of bolted connections in wood. Ph.D. dissertation, Department of Civil Engineering and Applied Mechanics, McGill University, Montreal
7. Kharouf N, McClure G, Smith I (2003) Elasto-plastic modeling of wood bolted connections. Comput Struct 81:747–754
8. Foschi RO, Bonac T (1977) Load–slip characteristics for connections with common nails. Wood Sci 9:118–123
9. Hong J (2007) Three-dimensional nonlinear finite element model for single and multiple dowel-type wood connections, Ph.D dissertation, Department of Wood Science, The University of British Columbia, Vancouver
10. Hong J, Barrett D (2010) Three-dimensional finite element modeling of nailed connections in wood. J Struct Eng ASCE 136:715–722
11. Finckenstein G (1999) Earthquake-resistant connections for post-and-beam timber construction. The research report, Department of Wood Science, The University of British Columbia, Vancouver
12. ANSYS Inc. (2006) Theory reference, ANSYS Release 8.0 help documentation, Swanson Analysis Systems, Canonsburg, PA
13. Forest Products Laboratory (1999) Wood handbook – wood as an engineering material. General Technical Report, FPL-GTR-113. FPA, Madison, WI
14. American Society for Testing and Materials (2007) Annual Book of ASTM Standards, Section 4 – Construction, Volume 04.10 Wood. ASTM international, West Conshohocken, PA
15. Saliklis EP, Urbanik TJ, Tokyay B (2003) Bilinear modelling of cellulosic orthotropic nonlinear materials. J Pulp Paper Sci 29:407–411
16. Smith I (1983) Coefficient of friction value applicable to contact surfaces between mild steel connectors such as bolts and dry European white wood. J Inst Wood Sci 9:229–234